Iron Metabolism and Cell Membranes

III. Iron-Induced Alterations in HeLa Cells

H. O. Jauregui, MD, W. D. Bradford, MD, A. U. Arstila, MD, T. D. Kinney, MD, and B. F. Trump, MD

The morphologic characteristics of acute iron loading were studied in HeLa cells incubated in an iron-enriched Eagle's medium containing 500 μg/ml of iron. Chemical studies showed that ferritin synthesis was rapidly induced and the concentration of intracellular ferritin increased up to 72 hours. Closely coupled with an increase in HeLa cell ferritin was a marked decrease in the rate of cell multiplication. The significant ultrastructural findings of iron-induced HeLa cell injury are characterized by the appearance of both autophagic multivesicular and residual bodies over the first 72 hours of iron incubation. The prominence of multivesicular bodies was noted after only 4 hours' incubation, with iron and myelin figures first appearing after 6 hours. Thus, the partial arrest of cell multiplication was associated with an increase in cytoplasmic residual bodies containing iron and other debris. The distribution of intracellular ferritin within HeLa cells differs significantly from the distribution described previously in hepatic parenchymal cells. In HeLa cells, ferritin particles were confined to lysosomal vesicles and were not identified in cell sap, endoplasmic reticulum, or Golgi apparatus.
(Am J Pathol 80:33–52, 1975)

CLINICAL OBSERVATIONS and animal experiments have demonstrated that iron overload in the body can be brought about by excessive oral iron intake,[1] disorder in mucosal regulation of iron absorption,[2] or parenteral injection of iron.[3,4] Once in the body, excess iron is stored chiefly in hepatic parenchymal cells and in the reticuloendothelial system. One complication of excess cellular iron appears to be damage to parenchymal cells but little or no damage to reticuloendothelial cells. This statement is based in part on evidence of remission of organ functional impairment and symptomatology following removal of iron by phlebotomy in cases of hemochromatosis and hemosiderosis, and in part on morphologic studies.[5] Necrotizing enteritis and hepatic necrosis following the ingestion of large amounts of ferrous sulfate provide additional evidence of cell damage by excess iron.[6,7] In spite of this data, it has not been possible to determine the sequence of destructive cellular changes, and the present information regarding the effect of iron on cells in chronic

From the Department of Pathology, Duke University Medical Center, Durham, North Carolina, and the Department of Pathology, University of Maryland School of Medicine, Baltimore, Maryland.
Supported by Grant GM-18273 from the US Public Health Service.
Accepted for publication February 25, 1975.
Address reprint requests to Dr. W. D. Bradford, Department of Pathology, Duke University Medical Center, Durham, NC 27710.

iron overload is confusing. This is due in part to the lack of a good animal model that adequately mimics iron storage disorders.

The use of a tissue culture system has many advantages for the study of the basic intracellular mechanisms of iron absorption, transport, and secretion. Such a system offers the notable advantage of having one population of cells in a controlled environment with the associated opportunity for pulse labeling. The present study demonstrates the morphologic consequences of acute iron loading in single cells and suggests possible pathways of intracellular iron transport as well as mechanisms of cell damage. The HeLa cell model was selected for these studies because of relative uniformity of cell population and because HeLa cells normally contain little endogenous iron but rapidly synthesize ferritin when molecular iron is added to the medium.[8]

Materials and Methods

Tissue Culture

HeLa cells were obtained from the American Type Culture Collection (CCL-2) and grown in monolayers by biweekly transfer following trypsinization. The experimental sublines coming from pooled cells were discarded after 45 days' activity and replaced by cells in the logarithmic growth phase. Cell cultures which were crowded and confluent were eliminated from the experimental design. Cultures were checked for *Mycoplasma* contamination by bacteriologic and ultrastructural monitoring. A cloned line of cells was used in multiple studies without variance in results. The population doubling time of the cells used in these experiments was 24 ± 2 hours.

Media

HeLa cells were grown in plastic flasks (T_{80} Falcon) at 30 C in Eagle's minimal essential medium (MEM Difco) with 10% fetal calf serum (FCS), in the fluid phase (MEM + 10% FCS), and 5% CO_2 and 95% O_2 in the gas phase. The powdered medium was dissolved in deionized water and sterilized by filtration, and penicillin (100 units/ml) and streptomycin (100 μg/ml) were added prior to use. Iron content of the complete medium was 0.27 μg Fe/ml by atomic absorption spectrometry.

Incubation with Iron-Supplemented Media

HeLa cell cultures were initiated by inoculating approximately $1 \times 10^5 \pm 0.3$ viable cells/Falcon flask. Less than 1×10^3 cells in the initial inoculum were dead. After these cells had grown for 12 to 18 hours in the tissue culture medium described previously, the medium was replaced with fresh MEM + 10% FCS in all cultures. In one-half of the cultures, this medium was supplemented with ferrous sulfate so that the final concentration of iron was 500 μg of iron/ml of medium. In the other half of the flasks, distilled water was added in quantities equal to that used in the ferrous sulfate solution. The pH was monitored in both lines of cells during the whole experiment and adjusted to 7.2 when required. Confluent growth was never reached in control or iron-incubated cells.

Electron Microscopy

Replicate cultures of control and iron-incubated cells were fixed for electron microscopy at hourly intervals by replacing the growth medium with 2% glutaraldehyde in 0.1 M

sodium cacodylate buffer at pH 7.4 (471 mOsmoles/liter). The fixation times, procedures of dehydration, and embedding are described elsewhere.[9] Thin sections were stained with uranyl acetate. Omission of the lead citrate facilitated visualization of ferritin.

Demonstration of acid phosphatase was accomplished with Gomori's lead phosphate technique [10]; incubation was performed at room temperature for 30 to 120 minutes. Thin sections also were studied unstained under the electron microscope.

Viability Studies

Five experiments were conducted in which cells were evaluated at 0, 6, 12, 24, 36, 48, 60, and 72 hours. At each time interval, three Falcon flasks of iron-incubated cells and three Falcon flasks of control cells were counted, a total of 42 flasks/experiment (including 6 flasks for zero time). Replicate cultures of control and iron-treated cells were detached in the following manner. The incubation medium was withdrawn and preserved after gentle shaking to remove dead cells; the cell monolayers were detached from the dishes by trypsinization for 15 minutes and the preserved incubation medium returned immediately to the dishes by gentle pipetting. This procedure was monitored using a phase-contrast inverted microscope, and trypsin was always withdrawn prior to detachment of the cell monolayers. Death of cells during detachment by trypsinization proved negligible in comparison to mechanical methods of detachment. In performing cell counts, both living and dead cells were counted. Dead cells were identified by their characteristic staining with erythrosin B; 0.1 ml of erythrosin B was added to 1 ml of cell suspension, and a minimum of 1000 cells were counted in a hemocytometer chamber.

Chemical Analysis

Determinations of protein, ferritin iron, and total iron were made from HeLa cells following suspension in Earle's basic salt solution at intervals over 72 hours. Protein was determined by the method of Lowry.[11] Ferritin and total iron levels in HeLa cells were determined by the method of Drysdale and Munro.[12] These methods are modifications of Hill's bipyridyl method [13] for the estimation of iron in the ferrous state and the Laufberger procedure for precipitating tissue ferritin.[14]

Results

Biochemical Findings

Total iron and ferritin iron were measured at intervals over a period of 72 hours in control and iron-stimulated monolayers of HeLa cells (Text-Figure 1). Total iron and ferritin iron levels in control cells did not change appreciably over the 72-hour time period studied. In contrast, the cells stimulated by incubation with ferrous sulfate demonstrated increased levels of both total iron and ferritin iron. Ferritin iron in iron-stimulated HeLa cells increased from 0.3 μg ferritin iron/mg of protein at zero time to 2.5 μg ferritin iron/mg protein at 72 hours. The increase in total iron content of the ferrous-sulfate-incubated cells was most marked between zero time and 6 hours, increasing from 0.7 to 10 μg iron/mg of protein.

Viability Studies

Table 1 indicates the total number of cells, total living cells, total dead cells, and average values with standard deviations for five experiments. At

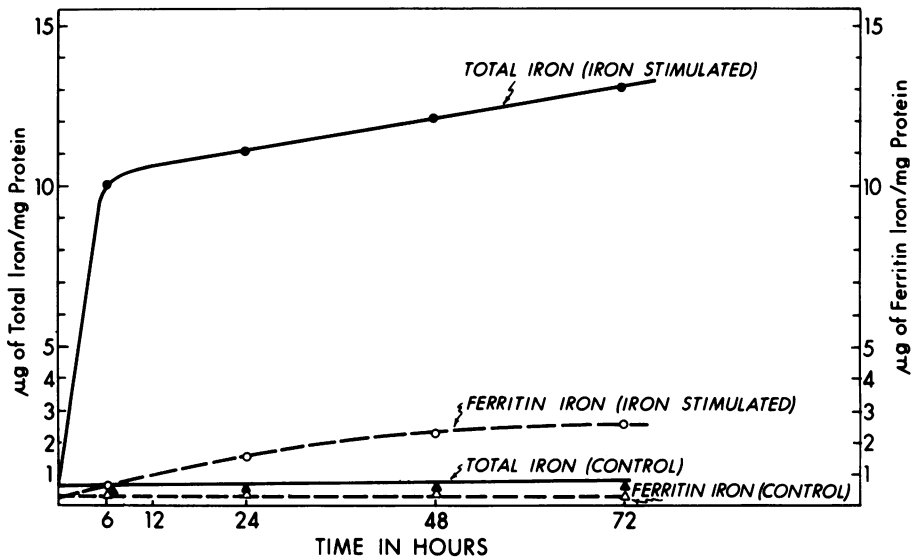

TEXT-FIGURE 1—Total iron and ferritin iron contents of control and iron-stimulated HeLa cells. Cells incubated with iron demonstrate an increase in both total iron *(solid lines)* and ferritin iron *(dotted lines)*.

each time interval, three Falcon flasks of iron-incubated cells and three Falcon flasks of control cells were counted, a total of 42 flasks/experiment.

After HeLa cells were grown in Eagle's modified media for 24 hours, 500 μg of ferrous sulfate/ml was added to one half of the culture flasks. When the rate of growth of HeLa cells in iron-enriched media and in control media was measured as a function of time and expressed as the total number of cells per flask, it is clear that the HeLa cells were growing in logarithmic fashion and never reached the stationary phase. When the number of living HeLa cells in both iron-enriched and control media were measured as a function of time and expressed as the number of living cells, the effects of ferrous sulfate on cell growth were apparent after 12 hours and were more marked after 24 and 72 hours. After 72 hours of growth, 8.7×10^5 cells were alive in control cultures, while the number of living cells in iron-enriched media was 3.7×10^5. After 24 hours, the number of dead cells in iron-supplemented media was 12.7% (0.24×10^5) while only 2.1% (0.06×10^5) dead cells were present in controls. After 48 hours of incubation, 19% (0.57×10^5) of iron-treated cells were dead, while only 2.3% (0.12×10^5) in the control were dead. By 72 hours, 24% (1.25×10^5) of the iron-treated cells were dead, while 5.6% (0.52×10^5) of the control cells were dead.

Electron Microscopy

Untreated Control Cells

The fine structure of the control polymorphous HeLa cell grown in Eagle's medium is pertinent to the interpretation of the present study. The cell membrane was smooth with short microvilli and occasional invaginations into the cytoplasm. Cisternae of rough surfaced endoplasmic reticulum were distributed throughout the cytoplasm but were not prominent. Profiles of smooth endoplasmic reticulum consisting of cisternae, vesicles, and vacuoles were scattered throughout the cytoplasm but were especially numerous around the Golgi area (Figure 1).

The extensive Golgi network lay near the nucleus. Relatively few multivesicular bodies were present. The typical multivesicular body was surrounded by small vesicles, limited by a single membrane, a part of which was often coated on the cytoplasmic side. Within the vacuole, a number of small uncoated vesicles of similar size were present. Approximately half of the multivesicular bodies appeared dark because of moderately electron-dense vesicles and matrix, while the others had a light appearance with light vesicles and matrix. The dark multivesicular bodies were regularly round, and the lighter ones were more irregular in shape. The uncoated vesicles adjacent to the multivesicular bodies measured approximately 400

Table 1—Viability Studies (Average of Five Experiments*)

Hours of culture		No. of cells $\times 10^5$ ($\pm$ SD)		
		Total	Living	Dead
0		1.20 ± 0.16	1.19 ± 0.17	0.02
12	Controls	2.00 ± 0.16	1.97 ± 0.15	0.03 ± 0.02
	Iron-incubated cells	1.70 ± 0.15	1.61 ± 0.14	0.09 ± 0.04
24	Controls	2.82 ± 0.19	2.76 ± 0.19	0.06 ± 0.03
	Iron-incubated cells	1.88 ± 0.21	1.64 ± 0.24	0.24 ± 0.06
36	Controls	3.93 ± 0.19	3.85 ± 0.21	0.08 ± 0.03
	Iron-incubated cells	2.60 ± 0.32	2.17 ± 0.36	0.41 ± 0.07
48	Controls	5.04 ± 0.40	4.92 ± 0.39	0.12 ± 0.02
	Iron-incubated cells	3.00 ± 0.10	2.42 ± 0.05	0.57 ± 0.05
60	Controls	7.02 ± 0.37	6.72 ± 0.37	0.30 ± 0.01
	Iron-incubated cells	4.25 ± 0.10	3.30 ± 0.16	0.95 ± 0.10
72	Controls	9.12 ± 0.47	8.71 ± 0.73	0.52 ± 0.13
	Iron-incubated cells	5.00 ± 0.44	3.75 ± 0.31	1.25 ± 0.25

* Experiment 3 was discontinued after 50 hours.

Å in diameter; the small ones measured 200 to 300 Å in diameter. In acid phosphatase preparations, there was lead phosphate reaction product in the matrical space of some multivesicular bodies near the Golgi apparatus, inner Golgi lamellae, vesicles, lysosomes, occasional profiles of endoplasmic reticulum, and nuclear envelope following the longest incubation periods. No ferritin particles were identified within the cytoplasm or cytocavitary network of these control cells. Myelin whorls and membranous debris were occasionally present in digestive vacuoles of young cells. As the cultures aged, there was an increase in multivesicular bodies and secondary lysosomes containing membranous debris after 72 hours of incubation. No ferritin was visualized in the older control cells. Autophagic vacuoles limited by double membranes were not prominent.

Iron-Incubated Cells

On addition of ferrous sulfate to the culture medium, a precipitate formed in the medium which was visible by electron microscopy in cells cultured for 12 or more hours. Amorphous fragments of this probable hydroxide or oxyhydroxide iron–protein complex, which were seen lying adjacent to the plasmalemma (Figure 7), were apparently taken up by endocytosis and passed to the lysosomal system. Within lysosomes, this complex was clearly distinguishable from ferritin aggregates by its amorphous, electron-dense mass and the lack of the particular micellar structure characteristic of ferritin particles in thin sections.[4,15]

Examination for ferritin in the sections of HeLa cells fixed at hourly intervals after incubation with iron showed that ferritin was first seen in sections taken at 4 hours and that ferritin could not be visualized in the sections taken at 1, 2, and 3 hours.

Four hours after incubation with iron, ferritin particles were first visualized within the matrix of single-membrane-limited lysosomes (Figure 2). Ferritin was not seen in the cell sap or various other parts of the cytocavitary network. The concentration of ferritin particles within lysosomes increased after 8, 12, 24, and 72 hours' incubation (Figures 3–6), and the ferritin particles were clearly distinguishable from other lysosomal debris because of their uniform size (70 Å) and typical cores (Figures 4 and 12). When monolayers of iron-treated HeLa cells were incubated for the demonstration of acid phosphatase, deposits of lead phosphate reaction product were seen within lysosomes containing ferritin.

HeLa cells incubated with iron for 6 to 8 hours showed a marked increase in multivesicular bodies. After 8 hours' incubation, ferritin particles were identified within the matrix of multivesicular bodies, and the con-

centration of ferritin and other dense irregular particles within these bodies increased through 72 hours. The formation of myelin-containing bodies was apparent following incubation with iron for 8 hours, and prominent myelin figures were well visualized at 24 (Figure 8), 48, and 72 hours (Figures 9 and 11). Thus, after 24 hours' incubation with iron, multivesicular bodies, digestive vacuoles with myelin figures, and residual bodies were prominent in iron-stimulated cells in contrast to control cells. After 48 hours' incubation, irreversible changes consisting of fragmentation and dissolution of cell membranes and organelles were present in many cells. After 24 hours' incubation, the lysosomes were filled with vesicles, follicular densities, membrane whorls, and nondescript amorphous material. Though particles of ferritin were still present, they were mixed with other irregular dense particles which probably represent some other form of hydroxide, oxyhydroxide iron–protein complex, or possibly hemosiderin (Figures 8 and 11).

By 72 hours, most residual bodies contained abundant dense particles, some of which were ferritin and others most likely representing different forms of iron oxide. At this time, ferritin or other iron precipitate could not be identified in the cytocavitary network or in other parts of the cell (Figures 9 and 11). By 72 hours, irreversible changes were seen in the great majority of the cells (Figure 10).

Discussion

The results of the present study show that when nonsynchronized HeLa cells in logarithmic growth phase are incubated in an iron-rich medium containing 500 μg/ml of iron, ferritin synthesis is rapidly induced and the concentration of intracellular ferritin continuously increases up to 72 hours. This finding is in accord with previous reports which indicate that iron induces appreciable ferritin synthesis within 2 hours.[8,16,17] Our results also show that, coupled with an increase in HeLa cell total iron content, there is a decrease in the rate of cell multiplication especially after 12 hours of iron incubation.

The present studies further demonstrate the morphologic progression of HeLa cell injury by iron which is characterized by the appearance of autophagic multivesicular and residual bodies. Multivesicular bodies were noted after only 4 hours' incubation, and myelin figures first appear after 6 hours. An increase in the autophagic process is well recognized as a sublethal form of cell injury.[18] In the physiologic "aging" process in stationary phase cultures, HeLa cells do increase their numbers of autophagic vacuoles but not to the extent that is seen following addition of iron to the medium.

The decrease in rate of cell multiplication was associated with an increase in residual bodies within the cytoplasm which contain iron as well as other debris. A correlation between an increase in number of residual bodies and mitotic arrest has been noted previously in eukaryotic cell cultures, and the two are probably related.[19] Thus, it is possible to ascribe the increased number of autophagic vacuoles to a reduction in cell division. An increase in the number of residual bodies could result either from increased formation or from decreased extrusion of these bodies. It is not known in the present case which situation obtained. It is possible that increased amounts of iron within the lysosome system stimulate the rate of intralysosomal digestion and so promote accumulation of debris-filled secondary lysosomes which, in turn, will produce an increased number of residual bodies. On the other hand, membrane damage may stimulate autophagy which, in turn, will produce an increased number of residual bodies.

While it is clear that iron exerts some adverse effects on HeLa cells, it is not clear how this effect is mediated. One way in which excessive amounts of iron could injure cells is by means of hastening lipid peroxidation reactions.[20-22] Recent studies have shown that iron in the ferrous state rapidly induces lipid peroxidation and characteristic morphologic changes of liver microsomes *in vitro*.[23,24] However, at the present time, we have been unable to induce lipid peroxidation in intact HeLa cells. Our preliminary observations suggest that the glycoprotein present in the trypsin-sensitive portion of the HeLa coat protects against peroxidation of whole cells.[25] Whether or not increased peroxidation is a sufficient stimulus to induce autophagocytosis is not presently known, although the preliminary findings suggest that this possibility should be studied further. It should be noted that lipid peroxidation has been implicated in the pathogenesis of so-called aging pigment which is thought to represent the gradual conversion by oxidation of lysosomal debris into the pigment lipofuscin.

In the present experiments the end-point of iron-induced cytotoxicity has been related to the point at which cells are no longer able to exclude erythrosin B and thereby remain unstained. Other studies suggest that uptake of this dye by injured cells is a late manifestation of cell response to toxic agents. When cultures of fibroblasts are subjected to a lethal dose of irradiation, the cells undergo progressive injury over a matter of hours. Delayed incorporation of radioactive thymidine is the first manifestation of toxicity and is followed by a) the inability of the cells to incorporate labeled uridine and phenylalanine, b) release of previously incorporated radioactive chromium and discharge of lysosomal enzymes, and finally, c) release of lactic dehydrogenase from the cell to the tissue culture medium

and the inability of the cells to exclude dyes.[26] Thus, using erythrosin B as a marker to determine cell death may not adequately reflect sublethal injury. On the other hand, sublethal cell injury is manifested by altered growth rates of HeLa cell cultures and ultrastructural abnormalities which have been described in the present studies.

The present study also demonstrates that the distribution of ferritin within HeLa cells clearly differs from that described in hepatic parenchymal cells following iron loading. From morphologic observation, the major difference in the HeLa cell is that ferritin particles are confined solely to lysosomal vesicles and cannot be identified in the cell sap, endoplasmic reticulum, or Golgi apparatus. The biosynthesis of ferritin in rat hepatocytes by free ribosomes is seven to twenty times greater than the ferritin production by membrane-attached ribosomes,[27] and our previous studies have shown that in liver cells a large pool of ferritin is distributed throughout the cell sap, although the concentration of ferritin is highest within lysosomes after parenchymal iron loading [4,15,28] Ferritin particles in liver cells are also visualized within profiles of the Golgi apparatus and occasionally in the endoplasmic reticulum. Confirmation of these observations must await fractionation studies in which cellular compartments and organelles of HeLa and liver cells are compared for their ferritin content. The visual localization of ferritin predominantly within lysosomes in HeLa cells is in accord with earlier findings by Richter, who demonstrated that most ferritin was localized inside membrane-limited vacuoles.[16] The possibility that ferritin is present in cell sap and is lost from HeLa cells during processing is not likely. When ferritin-loaded HeLa cells are subjected to photosensitization and then processed for electron microscopy by the method used in this study, an abundance of ferritin molecules released by lysosomes are visualized within the cell sap.[29]

We did not observe ferritin particles within lysosomes until after 4 hours' incubation in an iron-rich medium. However, the biochemical findings of Chu and Fineberg clearly indicate that ferritin synthesis begins within an hour after addition of iron to the tissue culture medium and that significant amounts of ferritin can be chemically detected by radioisotopes after 2 hours' incubation with iron.[8] The discrepancy between morphologic and chemical findings may be resolved if it is assumed that the rapidly synthesized ferritin is so low in molecular iron content as to be indiscernible by electron microscopy and that chemical methods detect very minute amounts of ferritin.

The pathway by which ferritin reaches the lysosomes in hepatic parenchymal cells is at present better understood than the pathway by which it is transported in HeLa cells. In liver cells we have shown that

some ferritin is apparently transported to lysosomes via the endoplasmic reticulum and Golgi apparatus and that ferritin also enters lysosomes by means of cellular autophagocytosis.[4,28] In HeLa cells we did not see ferritin particles in the cell sap, endoplasmic reticulum, and Golgi apparatus and so were unable to visualize a pathway by which ferritin is transported to lysosomes. There are at least three possible routes by which ferritin could enter the lysosomal system of the HeLa cells. The first possibility is that lysosomal ferritin is indeed derived from the endoplasmic reticulum–Golgi apparatus pathway. The observation that ferritin particles are always confined to the matrical space of the multivesicular bodies and do not appear inside the small vesicles supports this possibility. The second possibility is that ferritin enters the lysosomal pool by autophagocytosis from the HeLa cell sap. In autophagy it is understood that the smaller vesicles of the multivesicular bodies arise as buds from a small portion of the limiting multivesicular body membrane into the matrix.[9] Under this circumstance, we would expect to find ferritin particles inside the smaller vesicles, if indeed they are taken up from the cell sap by autophagocytosis. No ferritin particles were seen within small vesicles of multivesicular bodies in this study. The third possibility is that iron is transported directly into the lysosome, where it combines with apoferritin. This possibility would be compatible with the rapid appearance of discernible ferritin in the lysosomes if apoferritin, invisible in the electron micrographs of thin sections, is transported by either the first or second of the possible pathways to the lysosomes. In such a case, the iron would enter directly either by diffusion or by an active transport step at the lysosomal membrane and be added to apoferritin within the lysosome compartment, as was originally suggested by Richter.[16] This could explain the observation that ferritin is first visible in this compartment.

The differences in ferritin distribution within HeLa and liver cells are not explainable at this time. It is possible that these differences may be explained by the relative amounts of ferritin formed by the two cells. In the liver cell, the amount is very large, and although the cell sap contains abundant and easily visualizable ferritin, it is more concentrated in the lysosomes. In the HeLa cell, the amounts of ferritin are much lower, and the quantity in the cell sap is too small to be identified visually. The smaller amount of HeLa cell ferritin may be due to rate-limiting steps at the level of protein synthesis or at the level of the plasma membrane transport system.

Care must be exercised in differentiating the adverse effects of iron in liver and HeLa cells. Hepatic parenchymal cells are for the most part nonreplicating, while HeLa cells are mostly engaged in a continuous replica-

tion. It should be pointed out that cells growing in 95% O_2 and 5% CO_2, as in the present experiments, may behave quite differently than cells grown under other conditions. However, the adverse effect of iron in liver cell replication was also documented *in vivo* in rats previously subjected to partial hepatectomy.[30]

In conclusion, we have demonstrated that 500 μg/ml of iron affects the growth of HeLa cells in a negative manner when the cells are cultured under the specific conditions described in these experiments. The present data concerning adverse effects of iron on HeLa cells relate only to those cells that were able to adapt to 500 μg/ml of iron. It would be of interest to construct growth curves of the cells that were alive and replicating after 72 hours' iron incubation following transfer to a fresh iron-enriched medium. In future experiments the use of synchronized cells may suggest in which phase of the cell cycle iron exerts its most negative effect.

References

1. Kinney TD, Hegsted DM, Finch CA: The influence of diet on iron absorption. I. The pathology of iron excess. J Exp Med 90:137–146, 1949
2. Conrad ME, Weintraub LR, Crosby WH: The role of the intestine in iron kinetics. J Clin Invest 43:963–974, 1964
3. Goldberg L, Smith JP, Morten LE: The effects of intensive and prolonged administration of iron parenterally in animals. Br J Exp Pathol 38:297–311, 1957
4. Arstila AU, Bradford WD, Kinney TD, Trump BF: Iron metabolism and cell membranes. II. The relationship of ferritin to the cytocavitary network in rat hepatic parenchymal cells. Am J Pathol 58:419–449, 1970
5. MacDonald RA: Hemochromatosis and Hemosiderosis. Springfield, Ill, Charles C Thomas, 1964, pp 189–202
6. Witzleben C: An electron microscopic study of ferrous sulfate induced liver damage. Am J Pathol 49:1053–1067, 1966
7. Aldrich RA: Acute iron toxicity. Iron in Clinical Medicine. Edited by RO Wallerstein, SR Mettier. Berkeley, University of California Press, 1958, pp 93–104
8. Chu LLH, Fineberg RA: On the mechanism of iron-induced synthesis of apoferritin in HeLa cells. J Biol Chem 244:3847–3854, 1969
9. Arstila AU, Jauregui HO, Chang J, Trump BF: Studies on cellular autophagocytosis: Relationship between heterophagy and autophagy in HeLa cells. Lab Invest 24:162–174, 1971
10. Gomori G: Microscopic Histochemistry. Chicago, University Chicago Press, 1952
11. Lowry OH, Rosebrough NJ, Farr AL, Randall RJ: Protein measurement with the Folin phenol reagent. J Biol Chem 193:265–275, 1951
12. Drysdale JW, Munro HN: Small-scale isolation of ferritin for the assay of the incorporation of [^{14}C] labelled amino acids. Biochem J 95:851–858, 1965
13. Hill R: A method for the estimation of iron in biological material. Proc R Soc Med 107:205–214, 1930
14. Laufberger V: Sur la cristallisation de la ferritine. Bull Soc Chim Biol 19:1575–1584, 1937
15. Bradford WD, Elchlepp JG, Arstila AU, Trump BF, Kinney TD: Iron metabolism and cell membranes. I. Relation between ferritin and hemosiderin in bile and biliary excretion of lysosome contents. Am J Pathol 56:201–228, 1969

16. Richter GW: On ferritin and its production by cells growing in vitro. Lab Invest 12:1026–1039, 1963
17. Drysdale JW, Munro HN: Regulation of synthesis and turnover of ferritin in rat liver. J Biol Chem 241:3630–3637, 1966
18. Arstila AU, Trump BF: Studies on cellular autophagocytosis: The formation of autophagic vacuoles in the liver after glucagon administration. Am J Pathol 53:687–733, 1968
19. Richmond HG: The toxic effects of iron–dextrose complex on mammalian cells in tissue culture. Br J Cancer 15:594–606, 1961
20. Tappel AL, Zalkin H: Lipid peroxidation in isolated mitochondria. Arch Biochem Biophys 80:326–332, 1959
21. Tappel AL: Free-radical lipid peroxidation damage and its inhibition by vitamin E and selenium. Fed Proc 24:73–78, 1965
22. Dillard CJ, Tappel AL: Fluorescent products of lipid peroxidation of mitochondria and microsomes. Lipids 6:715–721, 1971
23. Hochstein P, Ernster L: Microsomal peroxidation of lipids and its possible role in cellular injury. Ciba Foundation Symposium, Cellular Injury. Edited by AVS de Reuck, J Knight. Boston, Little Brown and Company, 1963
24. Arstila AU, Smith MA, Trump BF: Microsomal lipid peroxidation: Morphological characterization. Science 175:530–533, 1972
25. Jackson S, Hayase K, Hanton J, Jauregui HO, Menzel DB.: Membrane structure as an antioxidant. Fed Proc 32:933, 1973
26. Houck JC: General introduction to the chalone concept. Chalones: Concepts and Current Researches. Natl Cancer Inst Monogr 38:1–4, 1973
27. Redman CM: Biosynthesis of serum proteins and ferritin by free and attached ribosomes of rat liver. J Biol Chem 244:4308–4315, 1969
28. Trump BF, Valigorsky JM, Arstila AU, Mergner WJ, Kinney TD: The relationship of intracellular pathways of iron metabolism to cellular iron overload and the iron storage diseases. Am J Pathol 72:295–356, 1973
29. Hawkins HK, Ericsson JLE, Biberfeld P, Trump BF: Lysosome and phagosome stability in lethal cell injury: Morphologic tracer studies in cell injury due to inhibition of energy metabolism, immune cytolysis and photosensitization. Am J Pathol 68:255–288, 1972
30. Valini FJ, Orfei E, Baserga R, Kent G: Effect of iron loading on parenchymal cell regeneration in the rat liver. Gastroenterology 48:515, 1965 (Abstr)

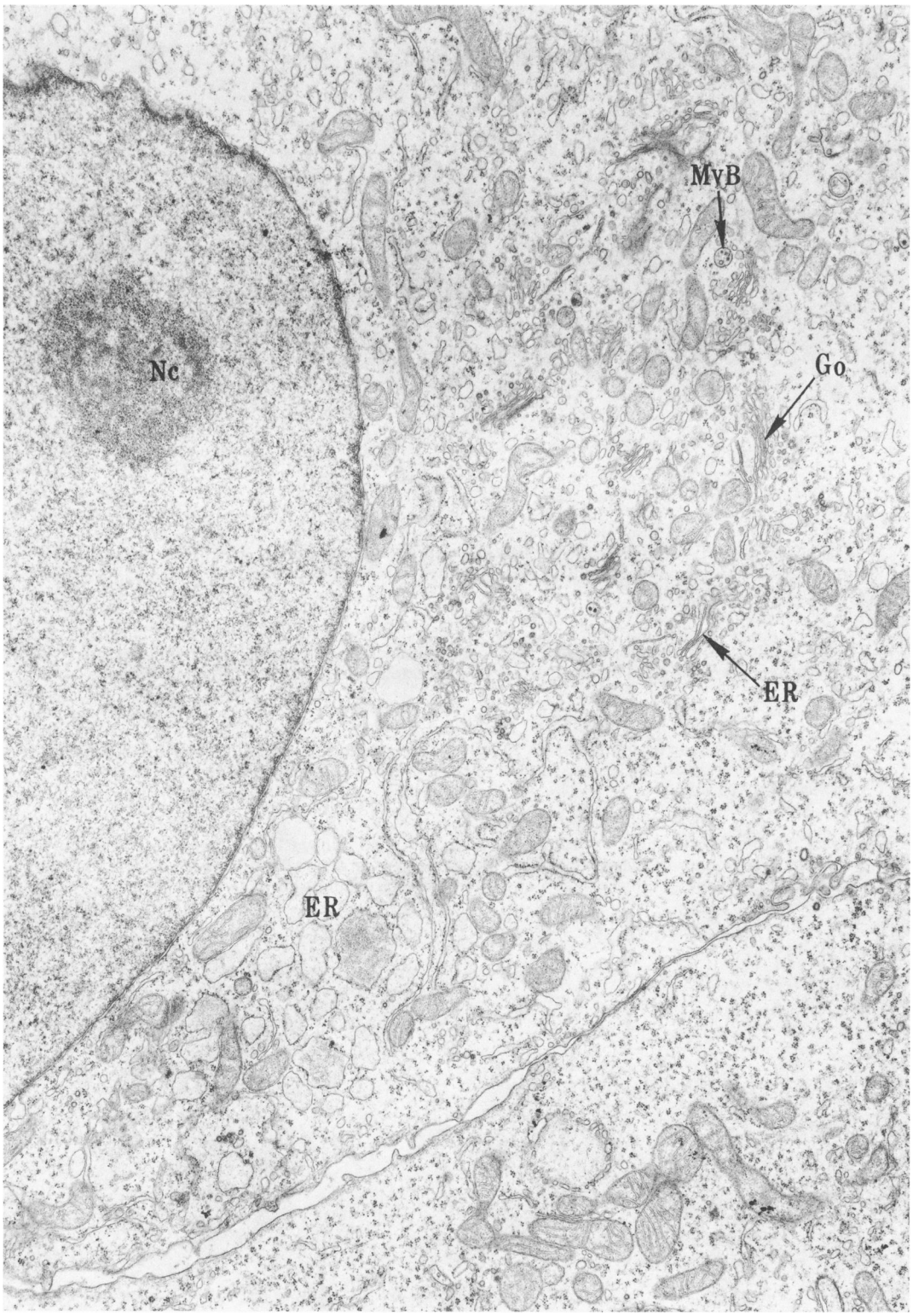

Figure 1—Electron micrograph shows portions of two control HeLa cells maintained in culture for 48 hours. Note the appearance of the nucleus and nucleolus (*Nc*) and the characteristic cytoplasmic organelles. The picture shows the Golgi region (*Go*), and numerous dictyosomes are seen cut in cross section among single-membrane-limited digestive vacuoles and multivesicular bodies (*MvB*). Note the numerous free polysomes and the small irregular mitochondria, and that some endoplasmic reticulum cisternae (*ER*) are dilated while others are collapsed. The cell membrane shows a few small microvilli. (× 9460)

Figure 2—Four-hour exposure to iron. Single-membrane-limited digestive vacuoles containing ferritin particles (*arrows*) along with scant debris. Note absence of ferritin in cell sap and nucleus (*N*). (× 120,000)

Figure 3—Eight-hour exposure to iron. Two multivesicular bodies showing ferritin in the matrix compartment (*arrow*). Note absence of ferritin in endoplasmic reticulum (*ER*) and cell sap. (× 120,000)

Figure 4—Twenty-four hours' exposure to iron. Single-membrane-limited digestive vacuoles containing ferritin particles (*arrows*) mixed with other debris. Again note absence of ferritin in cell sap. (× 151, 000)

Figure 5—Seventy-two hours' incubation with iron. Large multivesicular bodies containing vesicles, myelin figures, and ferritin. Note the absence of ferritin in the enclosed vesicles and note also its absence in the cell sap and endoplasmic reticulum (*ER*). (× 112,500)

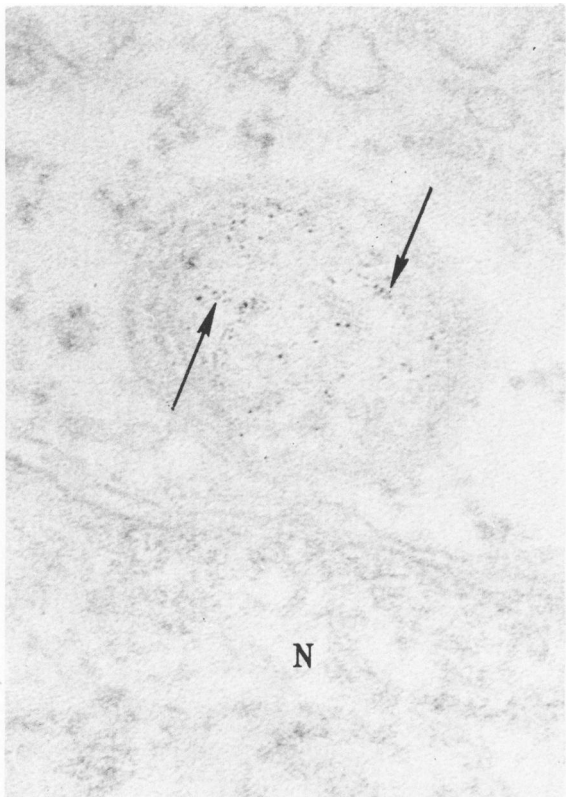

2

3

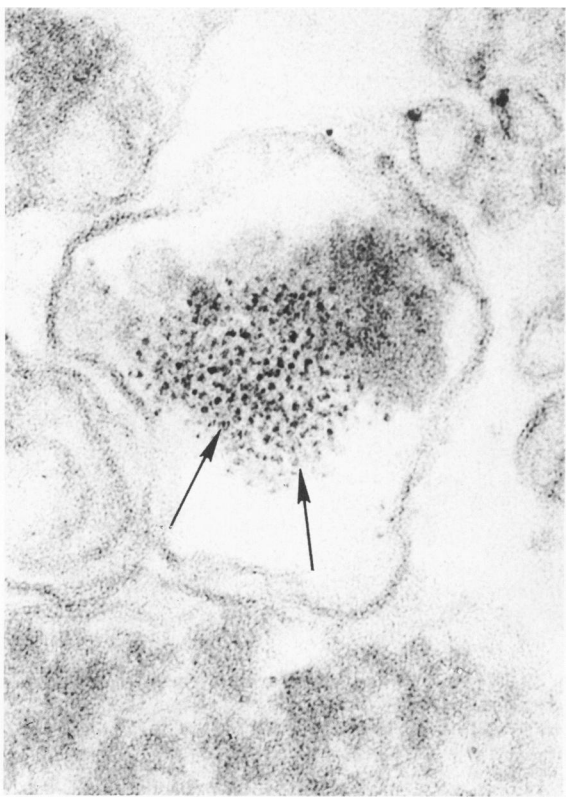

4

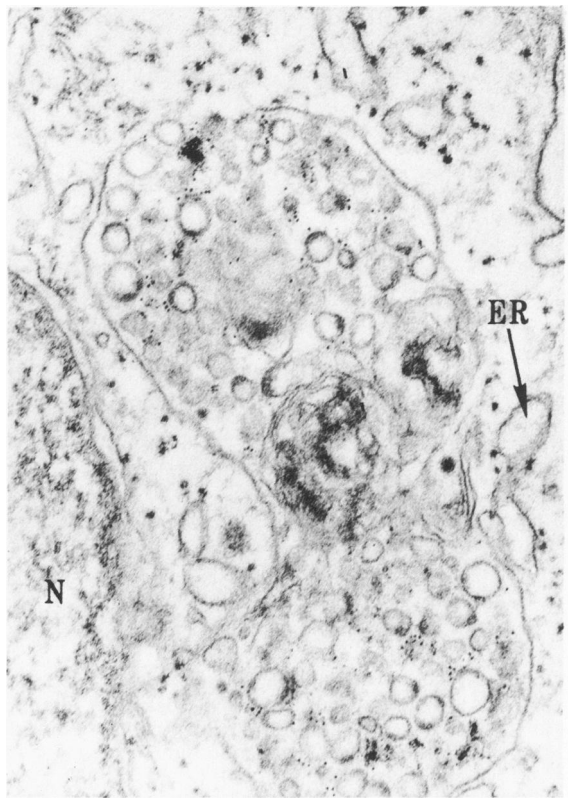

5

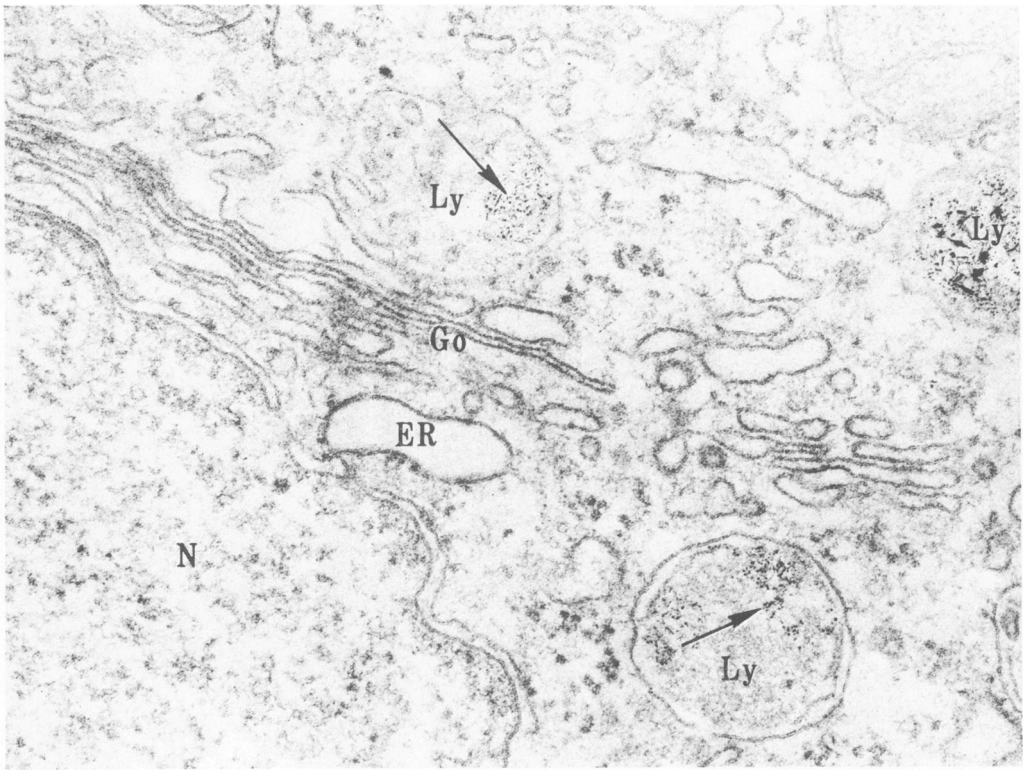

6

7

Figure 6—Twenty-four hours' exposure to iron. Golgi region (*Go*) showing three secondary lysosomes (*Ly*) containing clusters of ferritin (*arrows*). Note that the ferritin is not evenly mixed throughout the bodies, which contain other debris including vesicles and membrane fragments. Ferritin cannot be seen in the Golgi sacs themselves nor in the endoplasmic reticulum (*ER*), cell sap, or nucleoplasm (*N*). (× 80,000) **Figure 7**—Twenty-four hours' exposure to iron showing microvilli and HeLa cell surface. Note dense particles in intercellular space adherent to the cell membrane and in invaginations of it (*arrow*). These bodies are interpreted as iron precipitates formed by interaction with medium components. (× 130,000)

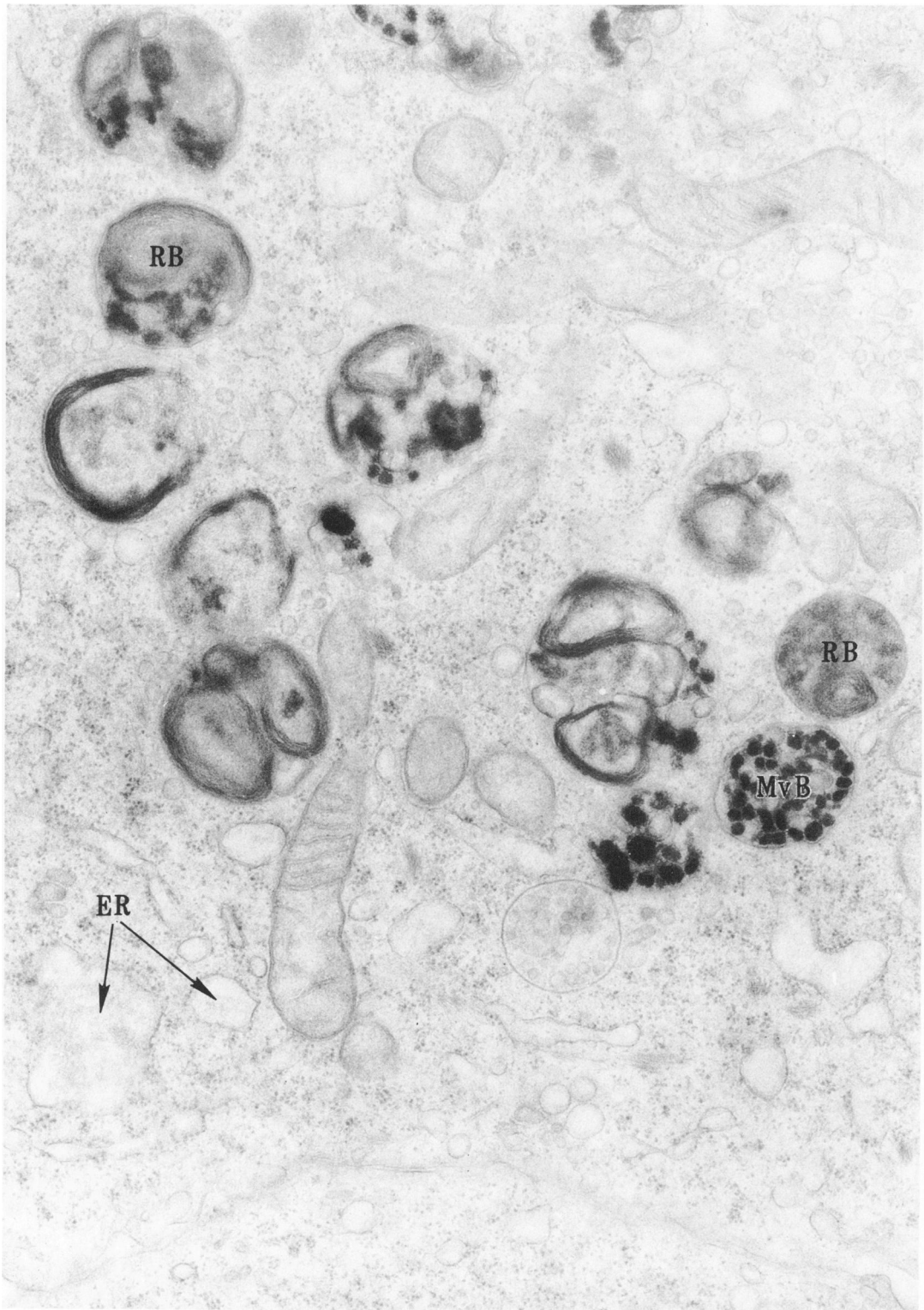

Figure 8—Twenty-four hours' exposure to iron. Area of cytoplasm showing multiple residual bodies (*RB*) and multivesicular bodies (*MvB*) filled with membranous and other debris and containing the dense precipitates referred to in Figure 7. Note absence of ferritin in mitochondria, endoplasmic reticulum (*ER*), and cell sap. (× 49,500)

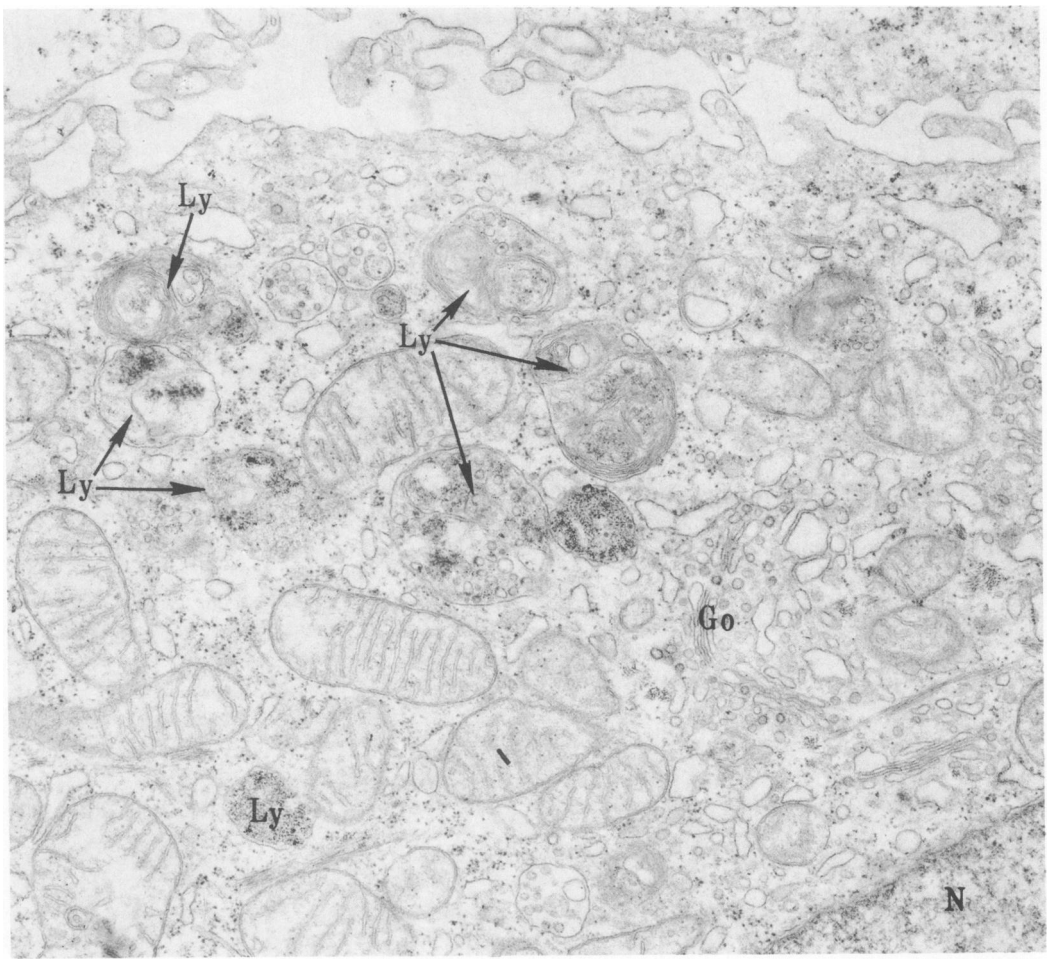

Figure 9—Seventy-two hours' exposure to iron. Golgi region (*Go*) showing several secondary lysosomes (*Ly*) containing ferritin (*arrows*). Other dense deposits possibly representing hemosiderin mixed with membranous debris are present within lysosomes. Note absence of ferritin in Golgi, endoplasmic reticulum, nucleoplasm, and cell sap. (× 46,000)

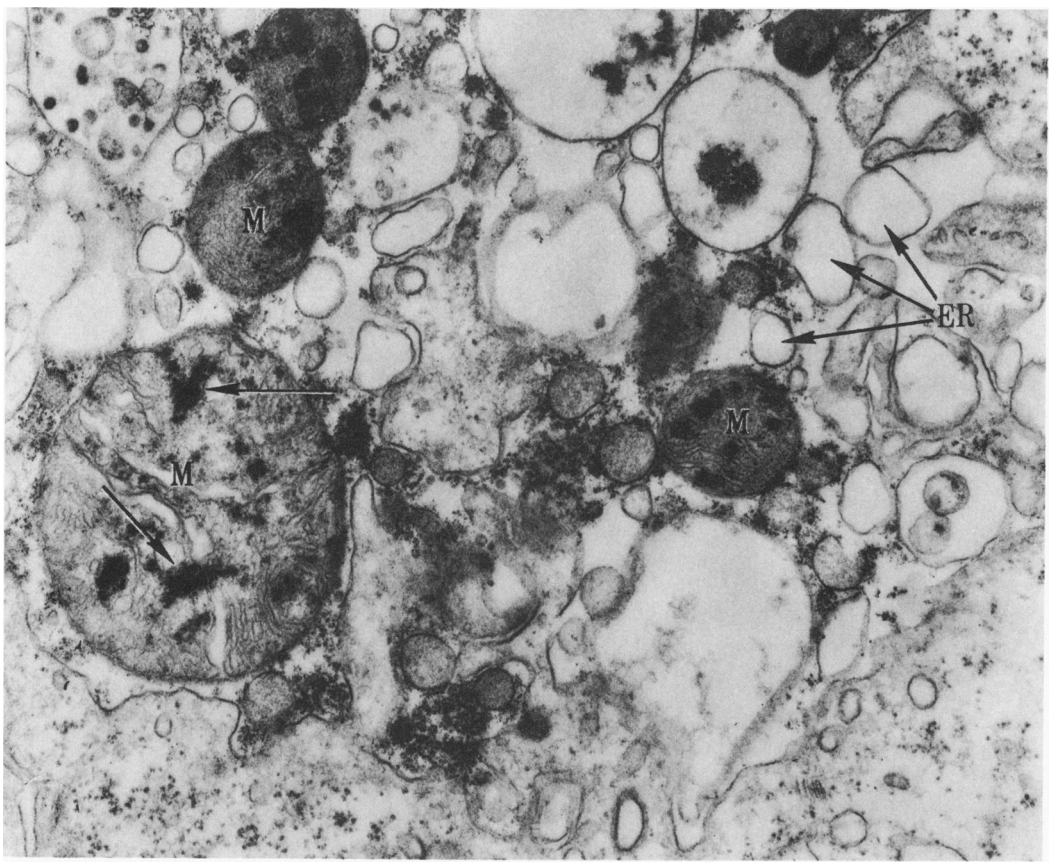

Figure 10—Seventy-two hours' exposure to iron. Portion of a necrotic cell showing characteristic mitochondria with flocculent densities (*arrows*) and dilated and fragmented endoplasmic reticulum (*ER*) and swollen cell sap. (× 85,000)

11

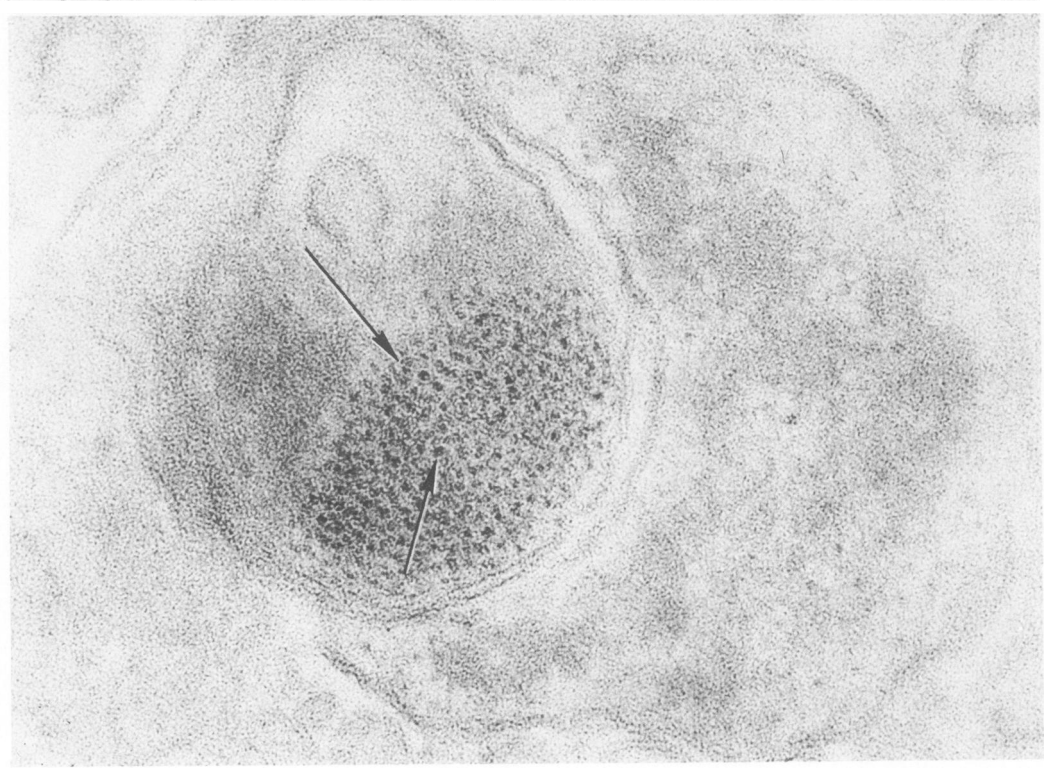

12

Figure 11—Exposure to iron for 72 hours. Two large secondary lysosomes (*Ly*) containing multiple vesicles, myelin figures, and scattered particles, some of which probably represent ferritin and hemosiderin (*arrows*). Note absence of ferritin in multivesicular bodies (*MvB*), cell sap, and mitochondria (*M*), and endoplasmic reticulum (*ER*). (× 75,000) **Figure 12**—Seventy-two-hour exposure to iron. Higher magnification of lysosome containing a cluster of ferritin particles (*arrows*), along with other membranous and nonmembranous debris. (× 160,200)